PHYSICAL REVIEW B **83**, 140402(R) (2011)

Nonresonant spin rectification in the absence of an external applied magnetic field

X. F. Zhu,[1,2] M. Harder,[2] J. Tayler,[2] A. Wirthmann,[2] B. Zhang,[1] W. Lu,[1,*] Y. S. Gui,[2,†] and C.-M. Hu[2]

[1]*National Laboratory for Infrared Physics, Shanghai Institute of Technical Physics, Chinese Academy of Sciences, Shanghai 200083, China*

[2]*Department of Physics and Astronomy, University of Manitoba, Winnipeg, Canada R3T 2N2*

(Received 22 November 2010; revised manuscript received 7 February 2011; published 12 April 2011)

A spin rectification effect due to the nonresonant magnetization motion has been found, which differs from the previously known spin rectification effect caused by the resonant magnetization precession at ferromagnetic resonance. A phase-resolved electrical detection technique has been used to measure the phase lag between the magnetization response and the driving microwave magnetic field, which demonstrates unambiguously the distinction between the resonant and nonresonant rectification effects.

DOI: 10.1103/PhysRevB.83.140402 PACS number(s): 76.50.+g, 75.78.−n, 85.75.−d, 42.65.−k

The spin rectification effect in a spin dynamo[1,2] originally refers to a time-independent field and current at the ferromagnetic resonance (FMR) generated by the nonlinear coupling[3] between (1) an oscillating resistance induced by a microwave magnetic field via anisotropic magnetoresistance (AMR) and (2) a microwave electric field e induced oscillating current j via Ohm's law. Due to its high sensitivity and measurement flexibility, the spin rectification effect has been successfully applied in the study of spin dynamics including FMR and/or spin wave resonances,[1,4–8] domain wall resonance,[9] as well as the nonlinear damping[10,11] in various kinds of ferromagnetic materials and structures. In addition, a comprehensive understanding of the spin rectification effect is also important to quantify the spin pumping effect[12] and the spin Hall effect[13,14] via electrical detection.

From a technical point of view, spin rectification obviously has the potential for broadband communication through the demodulation of amplitude modulated microwave signals by single ferromagnetic nanowires recently demonstrated by Yamaguchi *et al.*[15] Furthermore, since the spin rectification is extremely sensitive to the configuration of the microwave h field as well as the relative phase Φ between h and j waves,[16] the spin dynamo can also be utilized for h-vector detection[17] and phase-resolved microwave near-field imaging.[18]

However, the static magnetic field required for the resonances, on the order of a few 10 mT to a few 100 mT dependent on the microwave frequency, is not low, which significantly hinders these applications. Actually, such a resonant condition is not a prerequisite for spin rectification from a physics viewpoint. Consider the resistance of conduction materials under the superposition of a static magnetic field H and a dynamic magnetic field $\tilde{h} = h\exp(-i\omega t)$, which can usually be expanded as a Taylor series $\tilde{R}(\tilde{H} = H + \tilde{h}) \approx R(H) + h\exp(-i\omega t)d\tilde{R}/d\tilde{H}|_{\tilde{H}=H}$ at $|h/H| \ll 1$. Here the higher order h terms are omitted. Obviously, an oscillating resistance appears in general at nonresonant condition, and will ohmically couple with the dynamic current $\tilde{j} = j\exp(-i\omega t + i\Phi)$ ($j = S\sigma e$) excited by the microwave e field, where S and σ are the cross section and conductivity of samples, respectively, and Φ indicates the relative phase between e and h waves.[16] As a consequence, a nonzero dc photovoltage (PV) is generated according to

$$\begin{aligned} \mathrm{PV} &= \langle \mathrm{Re}(\tilde{j}) \cdot \mathrm{Re}(\tilde{R}) \rangle \\ &= \left\langle \mathrm{Re}(je^{-i\omega t + i\Phi}) \cdot \mathrm{Re}\left[he^{-i\omega t} \frac{d\tilde{R}}{d\tilde{H}}\bigg|_{\tilde{H}=H} \right] \right\rangle, \end{aligned} \quad (1)$$

where $\langle\rangle$ denotes the time average. Equation (1) amplifies the relevance of such a rectification effect from the original resonances in ferromagnetic materials and structures to any conductors with magnetoresistance no matter how it relates to spin dynamics or charge dynamics. In this Rapid Communication, we will demonstrate that indeed PV can be induced by a nonresonant motion such as the magnetization rotation (MR) or magnetization switching in a permalloy ($Ni_{80}Fe_{20}$, Py) microstrip. This enables a spin rectified voltage measured as $H \to 0$. To distinguish resonant and nonresonant rectification, phase-resolved PV spectroscopy is used to map the PV amplitude as functions of both Φ and H. Although both the nonresonant $\mathrm{PV_{MR}}$ due to magnetization rotation and the resonant $\mathrm{PV_{FMR}}$ at FMR due to the spin precession originating from the AMR effect, they show distinct differences under a phase-resolved measurement.

The primary experimental setup is shown in Fig. 1(a), where the key element is a second generation spin dynamo[10] including a coplanar waveguide (CPW) fabricated by a metallic bilayer of Cu/Cr (200/10 nm) and a Py microstrip with a dimension of $300 \times 7 \times 0.1\ \mu m^3$ underneath the short end of the CPW. Between them a 200 nm SiO_2 layer is used for electrical isolation. A microwave source is coherently split into two parts and injected into the CPW and Py microstrip. Finally, two microwaves with different phases due to the traveling length difference couple at the Py microstrip. Such a setup forms a spintronic Michelson interferometer.[18] A careful design makes it possible that in the Py microstrip the dominate h is from the CPW while the dominate j from another path.[18] Therefore the phase difference Φ between $\tilde{j}$ and $\tilde{h}$ in the Py microstrip can be effectively manipulated by a phase shifter inserted in one path. This enables a phase-resolved PV measurement. In the x-y-z coordinates shown in Fig. 1(a), the microwave current j is along z axis (the length of Py microstrip), the microwave magnetic field h is along x axis (the width of Py microstrip), and the static magnetic field **H**

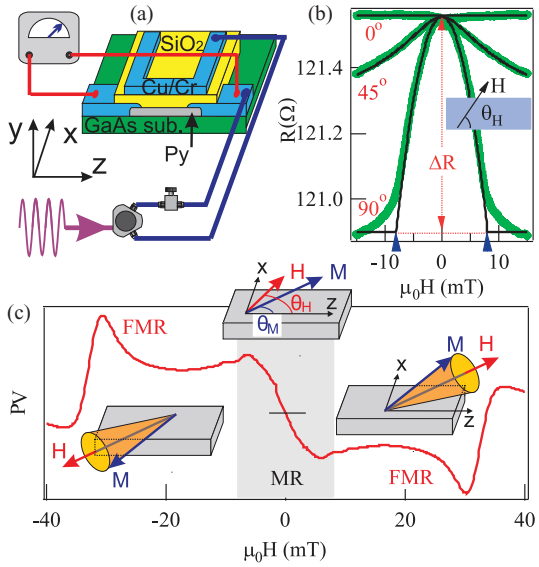

FIG. 1. (Color online) (a) The schematic diagram of the experimental setup, where the microwave power is split into two parts and forms a spintronic Michelson interferometer.[18] (b) Magnetoresistance for several orientations θ_H of H relative to the current direction. Arrows indicate the anisotropic field H_A. The open symbols are experimental data and solid curves are calculated using $R(0) = 121.53\ \Omega$, $\Delta R = 0.66\ \Omega$, and $H_A = 8.0$ mT. (c) A typical PV spectrum at $\theta_H = 75$ deg and $\omega/2\pi = 4.8$ GHz. Two kinds of motion have been indicated by the diagrams: magnetization rotation (MR) and magnetization precession at the FMR.

is applied in the x-z plane with an angle of θ_H relative to the z axis.

The microscopic origin of the AMR effect lies in the spin-orbit coupling and the resultant magnetoresistance follows a simple relation with the orientation of the magnetization $\mathbf{M}$ according to $R(H) = R(0) - \Delta R \sin^2\theta_M$, where $\mathbf{M}$ can be rotated by $\mathbf{H}$ according to $H_A \sin 2\theta_M = 2H \sin(\theta_H - \theta_M)$ (Ref. 19). H_A, indicated by the arrows in Fig. 1(b), is the anisotropic field determined by the demagnetization factor due to the shape of the Py microstrip, and θ_M, shown in Fig. 1(c), is the angle of $\mathbf{M}$ relative to the z axis. Figure 1(b) shows the measured magnetoresistance (symbols) for several θ_H, which agrees excellently with the calculation (solid curves) using $R(0) = 121.53\ \Omega$, $\Delta R = 0.66\ \Omega$, and $H_A = 8.0$ mT.

Under the radiation of microwave fields the magnetization angle $\tilde{\theta}_M$ becomes time dependent and results in an oscillating resistance. As a consequence, a typical PV spectrum in Fig. 1(c) shows a multi-origin rectification effect: magnetization precession at high fields and rotation at low fields, which will be verified in the latter discussion. Considering the pure magnetization rotation near $H = 0$, where $\theta_M \neq \theta_H$, $d\tilde{R}/d\tilde{H}$ should be determined by simultaneously solving the equations $H_A \sin 2\tilde{\theta}_M = 2\tilde{H} \sin(\theta_H - \tilde{\theta}_M)$ and $\tilde{R}(\tilde{H}) = R(0) - \Delta R \sin^2\tilde{\theta}_M$, where, in general, numerical calculation is necessary. However, we can easily conclude that $d\tilde{R}/d\tilde{H}$ is an odd function of H because $R(H)$ is an even function as shown in Fig. 1(b). A simple expression for the PV can be deduced

$$\mathrm{PV_{MR}} = -\frac{\Delta R j h H}{H_A^2} \cos\Phi, \tag{2}$$

at $\theta_H = 90°$, where $\sin\tilde{\theta}_M = \tilde{H}/H_A$ and $\mathrm{PV_{MR}} = 0$ at $\theta_H = 0°$. As expected $\mathrm{PV_{MR}}$ shown in both Figs. 1(c) and 2(a) is indeed an odd function of H, and furthermore it is almost linearly proportional to H near $H = 0$.

At $H \gg H_A$, the magnetization $\mathbf{M}$ is forced to align toward $\mathbf{H}$ and a microwave field $\tilde{h} = h\exp(-i\omega t)$ drives $\mathbf{M}$ to elliptically precess around $\mathbf{H}$. As a consequence it has been found that $\tilde{\theta}_M \sim \theta_H + \chi_{xx} h \cos\theta_H \exp(-i\omega t)\exp(i\Theta)/M_0$,[2] where $\chi_{xx} \sim M_0/\sqrt{(H - H_r)^2 + \Delta H^2}$ is the magnitude of the diagonal matrix element of the susceptibility tensor, $\Theta = \mathrm{arccot}[(|H| - |H_r|)/\Delta H]$ is the spin resonance phase, H_r is the FMR field, and ΔH is the line width of the FMR. In this case, the rectified PV can also be deduced according to Eq. (1), and is given by

$$\begin{aligned}\mathrm{PV_{FMR}} &= -\frac{\chi_{xx}\Delta R j h}{2M_0} \sin(2\theta_H)\cos\theta_H \cos(\Phi - \Theta) \\ &\approx -\frac{\Delta R j h}{2\Delta H} \sin(2\theta_H)\cos\theta_H [L\sin\Phi + D\cos\Phi],\end{aligned} \tag{3}$$

where $L = \Delta H^2/[(H - H_r)^2 + \Delta H^2]$ and $D = \Delta H(|H| - |H_r|)/[(H - H_r)^2 + \Delta H^2]$ represent the symmetric and antisymmetric Lorentz line shapes. Equation (3) implies that the origin of the complex line shape of the electrically detected FMR is the relative phase Φ.

Figure 2(a) shows typical PV spectra for several θ_H, which demonstrates unique features of $\mathrm{PV_{FMR}}$ such as $\mathrm{PV_{FMR}}(\theta_H) = -\mathrm{PV_{FMR}}(\theta_H + 180°)$ and $\mathrm{PV_{FMR}}(\theta_H = 0, 90, 180, \ldots,) = 0$, which can be well explained by Eq. (3). One can also use Eq. (3) to fit the line shape of the FMR. A good agreement can be achieved as shown in Fig. 2(a) with $\mu_0 H_r = \pm 22.7$ mT, $\mu_0 \Delta H = 3.5$ mT, and $\Phi = 0.87\pi$. The deduced frequency dependence of H_r at $\theta_H = 45°$ is plotted in Fig. 2(b), which exactly follows the relation of $\omega = \gamma\sqrt{|H_r|(M_0 + |H_r|)}$ with an effective gyromagnetic ratio of $\gamma/2\pi = 28.0\ \mu_0$ GHz/T and a saturation magnetization of $\mu_0 M_0 = 1.0$ T. Figure 2(c) shows the contribution of the symmetric and antisymmetric Lorentz line shapes to PV spectra as a function of θ_H, which can be well described by a $\sin(2\theta_H)\cos\theta_H$ function (solid and dashed curves).

Until now, there has not been direct evidence to prove that the structure near $H = 0$ must be caused by magnetization rotation. All the features near $H = 0$ may also be explained by a resonance. For this purpose a powerful phase-resolved PV measurement has been carried out and the spectra are plotted in Fig. 3(b). It demonstrates unambiguous resonant features[18] at $20\ \mathrm{mT} < \mu_0 H < 40\ \mathrm{mT}$ as discussed in detail below, while such resonant features do not exist at $H \approx 0$. More specifically, there are two main differences between resonant and nonresonant signals in the PV spectra shown in Figs. 3(a) [sweeping in the horizontal direction of Fig. 3(b)] and (c) [sweeping in the vertical direction of Fig. 3(b)], respectively. A resonant structure of FMR always exists no matter what value is the relative phase Φ. The value of Φ only determines the line shape of FMR as shown in

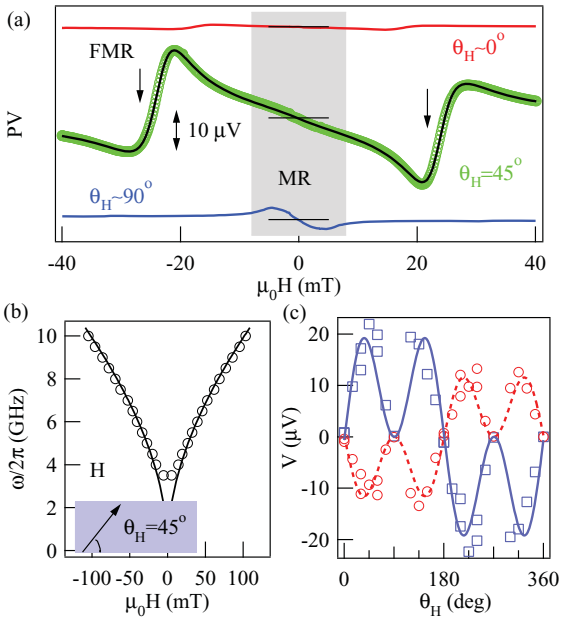

FIG. 2. (Color online) (a) Typical spectra of PV for several θ_H at $\omega/2\pi = 4.8$ GHz. For $\omega/2\pi = 45$ deg open symbols and the solid curve are experimental data and fitting results, respectively. (b) The frequency of FMR as a function of H at $\theta_H = 45$ deg. The solid curves are the calculation according to $\omega^2 = \gamma^2|H_r|(M_0 + |H_r|)$. (c) The deduced contribution of symmetric Lorentz line shape (circles) and antisymmetric Lorentz line shape (squares) as a function of θ_H at $\omega/2\pi = 4.8$ GHz, and the solid and dashed curves are $\sin(2\theta_H)\cos\theta_H$ functions.

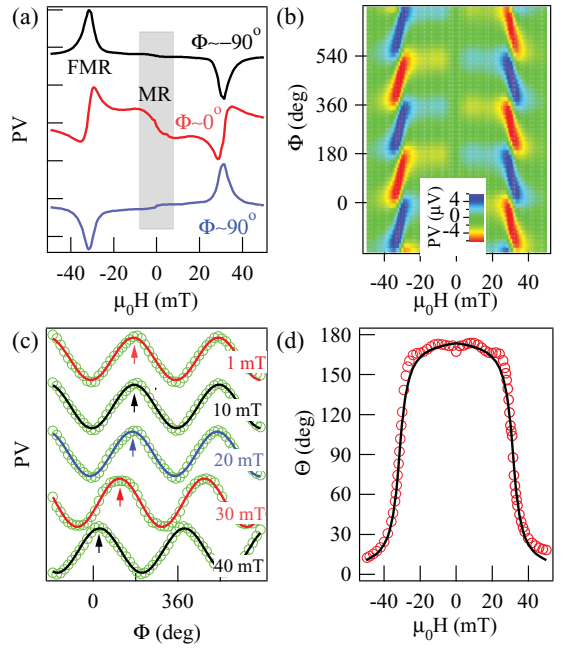

FIG. 3. (Color online) (a) PV spectra at $\Phi = -90$, 0, and 90 deg. The orientation of H is fixed at $\theta_H = 75$ deg. (b) Two-dimensional PV amplitude mapping by varying both H and Φ. (c) The normalized PV spectra as a function of Φ for several H. For clarity, the phase shift is indicated by the arrows. (d) Measured (symbols) and calculated (solid curves) ferromagnetic resonance phase Θ, that is, phase lag of the dynamic magnetization response relative to the driving h field, as a function of H.

Fig. 3(a): symmetric Lorentz line shape at $\Phi = n \cdot 180° + 90°$ and antisymmetric Lorentz line shape at $\Phi = n \cdot 180°$, where n is an integer. These features of FMR exactly follow Eq. (3). In contrast, PV near $H = 0$ does not change its line shape, and its amplitude reaches a maximum at $\Phi = n \cdot 180°$ and vanishes at $\Phi = n \cdot 180° + 90°$ following Eq. (2). The excellent agreement between the experimental results in Fig. 3(a) and the theoretical expression Eq. (2) proves that the PV feature near $H = 0$ is indeed $\mathrm{PV_{MR}}$ due to magnetization rotation and the participation of resonance can be therefore excluded.

Another evidence of $\mathrm{PV_{MR}}$ is from the directly measured phase lag. Fixing the applied H field and sweeping the phase Φ, the PV demonstrates an interference pattern strictly following a sinusoidal function as shown in Fig. 3(c). Obviously, the phase shows a dramatic change in the vicinity of FMR: almost 180° from $\mu_0 H = 40$ mT to $\mu_0 H = 20$ mT, which can be interpreted by the universal feature of a resonance: the phase of the response oscillation always lags behind that of the driving force.[20] The phase smoothly varies from 0° to 180° in a narrow range determined by the damping and passes through 90° at the resonance. In contrast, the nonresonant response is only in-phase following the driving force and is shown to be constant from $\mu_0 H = 20$ to $\mu_0 H = 1$ mT. To demonstrate the accuracy in the determination of phase lag by spintronic Michelson interferometry, the spin-resonance phase $\Theta = \mathrm{arccot}[(|H| - |H_r|)/\Delta H]$ from the solution of the Landau-Lifschitz-Gilbert equation of FMR is calculated using $H_r = 31.5$ and $\Delta H = 3.5$ mT, which have been previously deduced from fitting the line shape in an independent experiment. The calculation (solid curves) without any fitting parameters agrees remarkably well with the experimental data (open symbols) shown in Fig. 3(d).

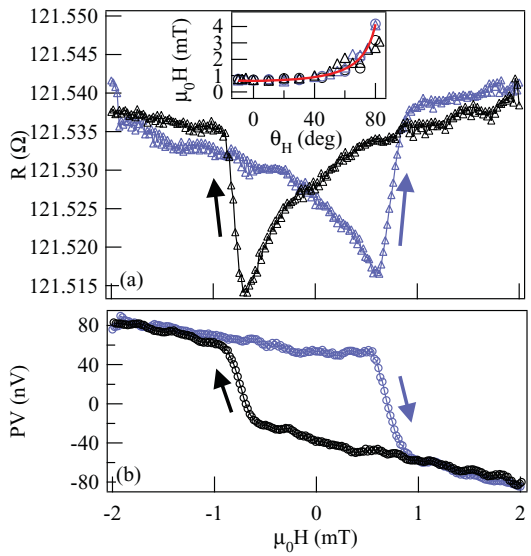

FIG. 4. (Color online) Magnetization switching detected by (a) resistance and (b) PV at $\theta_H = 0°$. Arrows indicate the sweeping direction of the H field. The inset shows the angular dependence of the switching field from R data (open triangles), PV data (open circles), and theoretical results based on the Kondorsky model (solid line) (i.e., $1/\cos\theta_H$ dependence).

Finally, we demonstrate the spin rectification due to magnetization switching, which can produce a nonzero PV even at $H = 0$. The magnetoresistance at $\theta_H = 0^\circ$ in Fig. 1(a) appears to be constant independent of H at first sight. However, a more careful examination reveals two dips appearing at $\sim\pm 0.7$ mT corresponding to magnetization switching in the microstrip, as shown in Fig. 4(a). Such a dip is characterized by a resistance change of about 0.02Ω [i.e., $\Delta R/R(0) \sim 0.016\%$]. Although $\Delta R/R(0)$ for magnetization switching is more than an order of magnitude smaller than the AMR effect $\Delta R/R(0) \sim 0.54\%$, the resultant PV is successfully used to monitor such a process characterized by a hysteresis loop of the PV curve, as shown in Fig. 4(b). This is compared with conventional resistance measurements for the electric detection of magnetization switching in Fig. 4(a), here the huge background due to sample resistance does not appear in PV measurements. The inset shows the angular dependence of the switching field for the resistance (open triangles) and PV (open circles) measurements, and both of them follow a $1/\cos\theta_H$ dependence (solid line). This indicates that the switching mechanism is the domain wall motion following the Kondorsky model,[21] where $H \ll H_A$ is insufficient to cause a uniform rotation of the magnetization away from the easy axis.

Notice the static resistance $R(H = 0)$ in Fig. 4(a) is not the extreme point of $R(H)(dR/dH = 0)$ differing from the case of the magnetization rotation shown in Fig. 1(b). According to Eq. (1) a nonzero PV must exist at $H = 0$ because $dR(0)/dH \neq 0$. Experimentally, as shown in Fig. 4(b) a nonzero PV appears at $H = 0$ and its polarization depends on the sweeping direction, which determines the sign of dR/dH. This implies that PV technique is applicable even in the absence of an external applied H field and therefore the barrier of an appropriate H field for the realistic applications is removed by nonresonant spin rectification.

In summary, we have demonstrated that the spin resonance is not a prerequisite for the generation of a PV signal due to microwave radiation, where PV technique has previously shown its high sensitivity in the study of spin dynamics. In general, PV technique can be applied to most metals and semiconductors in a broad H range, in which the resistance is a function of the applied static magnetic field rather than a constant. Regarding dR/dH being larger in semiconductors, very recently people have begun to use semiconductor-ferromagnetic metal hybrid structures to study spin dynamics and find that the PV measurements provide a sensitive and noninvasive tool for probing the spin waves of nanomagnets.[22] It is therefore believed that PV technique possesses unprecedented capabilities for nonlinear conducting materials such as semiconductors in the vicinity of the quantum Hall regime or superconductors close to T_c, where dR/dH is giant.

We thank G. E. Bridges, W. J. Jiang, and G. Roy for discussions and technical support. This work has been funded by NSERC, CFI, CMC, and URGP grants (C.-M. H), and National Natural Science Foundation of China Grant No.10990100 (W.L).

*luwei@mail.sitp.ac.cn

†ysgui@physics.umanitoba.ca

[1] Y. S. Gui, N. Mecking, X. Zhou, G. Williams, and C.-M. Hu, Phys. Rev. Lett. **98**, 107602 (2007).

[2] N. Mecking, Y. S. Gui, and C.-M. Hu, Phys. Rev. B **76**, 224430 (2007).

[3] H. J. Juretschke, J. Appl. Phys. **31**, 1401 (1960).

[4] A. A. Tulapurkar, Y. Suzuki, A. Fukushima, H. Kubota, H. Maehara, D. D. Djayaprawira, N. Watanabe, and S. Yuasa, Nature (London) **438**, 339 (2005).

[5] A. Yamaguchi, H. Miyajima, T. Ono, Y. Suzuki, S. Yuasa, A. Tulapurkar, and Y. Nakatani, Appl. Phys. Lett. **90**, 182507 (2007).

[6] Y. S. Gui, N. Mecking, and C.-M. Hu, Phys. Rev. Lett. **98**, 217603 (2007).

[7] A. Yamaguchi, K. Motoi, A. Hirohata, H. Miyajima, Y. Miyashita, and Y. Sanada, Phys. Rev. B **78**, 104401 (2008).

[8] V. A. Atsarkin, V. V. Demidov, L. V. Levkin, and A. M. Petrzhik, Phys. Rev. B **82**, 144414 (2010).

[9] D. Bedau, M. Kläui, S. Krzyk, U. Rüdiger, G. Faini, and L. Vila, Phys. Rev. Lett. **99**, 146601 (2007).

[10] Y. S. Gui, A. Wirthmann, N. Mecking, and C.-M. Hu, Phys. Rev. B **80**, 060402(R) (2009).

[11] C. T. Boone, J. A. Katine, J. R. Childress, V. Tiberkevich, A. Slavin, J. Zhu, X. Cheng, and I. N. Krivorotov, Phys. Rev. Lett. **103**, 167601 (2009).

[12] M. V. Costache, M. Sladkov, S. M. Watts, C. H. van der Wal, and B. J. van Wees, Phys. Rev. Lett. **97**, 216603 (2006).

[13] O. Mosendz, J. E. Pearson, F. Y. Fradin, G. E. W. Bauer, S. D. Bader, and A. Hoffmann, Phys. Rev. Lett. **104**, 046601 (2010).

[14] L. Liu, T. Moriyama, D. C. Ralph, and R. A. Buhrman, Phys. Rev. Lett. **106**, 036601 (2011).

[15] A. Yamaguchi, H. Miyajima, S. Kasai, and T. Ono, Appl. Phys. Lett. **90**, 212505 (2007).

[16] J. D. Jackson, *Classical Electrodynamics*, 2nd ed. (John Wiley & Sons, New York, 1975).

[17] L. H. Bai, Y. S. Gui, A. Wirthmann, E. Recksiedler, N. Mecking, C.-M. Hu, Z. H. Chen, and S. C. Shen, Appl. Phys. Lett. **92**, 032504 (2008).

[18] A. Wirthmann, X. Fan, Y. S. Gui, K. Martens, G. Williams, J. Dietrich, G. E. Bridges, and C.-M. Hu, Phys. Rev. Lett. **105**, 017202 (2010).

[19] B. A. Kalinikos and A. N. Slavin, J. Phys. C: Solid State Phys. **19**, 7013 (1986).

[20] L. D. Landau and E. M. Lifshitz, *Mechanics*, 2nd ed. (Pergamon Press, Oxford, 1969).

[21] E. Kondorsky, J. Phys. (Moscow) **2**, 161 (1940).

[22] P. Saraiva, A. Nogaret, J. C. Portal, H. E. Beere, and D. A. Ritchie, Phys. Rev. B **82**, 224417 (2010).